Hindawi
Mathematical Problems in Engineering
Volume 2023, Article ID 5401372, 12 pages
https://doi.org/10.1155/2023/5401372

Research Article

Prediction of Flank Wear during Turning of EN8 Steel with Cutting Force Signals Using a Deep Learning Approach

S. K. Thangarasu,[1] **T. Mohanraj**,[2] **K. Devendran**,[3] **M. Rajalakshmi**,[4] **Subrata Chowdhury**,[5] **and Saravanakumar Gurusamy**[6]

[1]*Department of Mechatronics Engineering, Kongu Engineering College, Erode, Tamilnadu, India*
[2]*Department of Mechanical Engineering, Amrita School of Engineering, Amrita Vishwa Vidyapeetham, Coimbatore, India*
[3]*Department of Computer Science Engineering, Kongu Engineering College, Erode, Tamilnadu, India*
[4]*Department of Biomedical Engineering, Sethu Institute of Technology, Virudhunagar, Tamilnadu, India*
[5]*Department of Computer Science and Engineering, Sreenivasa Institute of Technology and Management Studies, Chittoor, Andhra Pradesh, India*
[6]*Department of Electrical and Electronics Technology, FDRE Technical and Vocational Training Institute, Addis Ababa, Ethiopia*

Correspondence should be addressed to S. K. Thangarasu; skthangarasu@gmail.com and Saravanakumar Gurusamy; saravanakumar.gurusamy@etu.edu.et

Received 24 August 2022; Revised 15 October 2022; Accepted 17 October 2022; Published 15 February 2023

Academic Editor: Chaoqun Duan

Currently, manufacturing industries focus on intelligent manufacturing. Prediction and monitoring of tool wear are essential in any material removal process, and implementation of a tool condition monitoring system (TCMS) is necessary. This work presents the flank wear prediction during the hard turning of EN8 steel using the deep learning (DL) algorithm. The turning operation is conducted with three levels of selected parameters. CNMG 120408 grade, TiN-coated cemented carbide tool is used for turning. Cutting force and flank wear are assessed under dry-cutting conditions. DL algorithms such as adaptive neuro-fuzzy inference system (ANFIS) and convolutional auto encoder (CAE) are used to predict the flank wear of the single-point cutting tool. The DL model is developed with turning parameters and cutting force to predict flank wear. The different ANFIS and CAE models are employed to develop the prediction model. Grid-based ANFIS structure with Gauss membership function performed better than ANFIS models. The ANFIS model's average testing error of 0.0074011 mm and prediction accuracy of 99.81% are achieved.

1. Introduction

The required component can be manufactured through conventional and unconventional machining processes [1, 2]. Automated industries focus on conventional machining processes such as turning, milling, and grinding. Tool wear monitoring is essential to enhance product quality during the machining process. To monitor the machining process with high precision, the tool condition monitoring system (TCMS) should be an integral part of the automated manufacturing systems. TCMS can enhance production and enrich the performance of the machining system by improving the tool life, diminishing downtime and scrappage, and avoiding damage through continuous monitoring and predictive analysis [3]. Tool condition has been monitored by measuring the various sensor signals like cutting force, vibration [4], and sound signals [5]. Cutting force (CF) can be measured with piezoelectric or strain gauge-based sensors [6, 7]. The I-Kaz method analyzed a low-cost strain gauge sensor that measured the CF signals. The investigational outcomes were compared with the adaptive neuro-fuzzy inference system (ANFIS) based prediction model, which produced a maximum of 5.08% error [8]. The ANFIS model with "gbellmf" was used to forecast the surface roughness in milling operation by considering the spindle speed, feed, and depth of cut as input parameters [9].

Tool wear is more sensitive to CF signals, and CF signals are used to indicate tool conditions. Also, CF signals are gradually increased with a rise in tool wear. CF is measured directly through a dynamometer, and the tool wear is measured indirectly by analyzing the CF signals [10]. Prediction of tool wear and optimization of drilling parameters were carried out by ANFIS and genetic algorithm (GA), respectively. A smaller feed was suggested to minimize the thrust force and torque [11]. Response surface methodology (RSM) was employed to investigate process parameters' effects on CF, surface roughness (Ra), and cutting temperature. Out of two forecasting models, such as an artificial neural network (ANN) and ANFIS, the ANFIS model predicts the response more accurately. The optimum process parameters were selected using the RSM [12].

Estimation of tool life was carried out by the ANFIS model using the surface roughness and CF. The accuracy of the proposed model was 92.62% [13]. ANFIS model was used to estimate the material removal rate (MRR) and surface roughness (Ra) while turning stainless steel 202. The depth of cut and spindle speed was found as the most influencing parameter for MRR and Ra, respectively [14]. CF was estimated using ANFIS with spindle speed, feed, and depth of cut during the turning process, and the CF was predicted with an average error of 2.59% [15].

The neural network was used to forecast the CF, Ra, and tool wear while turning the CP-Ti grade II workpiece. The proposed model was suitable for predicting the responses within a 5% error [16]. A discrete and continuous monitoring, hybrid policy-based tool replacement mechanism was developed. The hybrid policy was optimized by particle swarm optimization (PSO) algorithm. All policies' results were analyzed, and PSO performed better than the others [17]. Online monitoring of grinding wheel wear was investigated in the grinding of Ti-6Al-4V titanium alloy. The result indicated that the Gaussian membership function-based ANFIS model was more intelligent for monitoring the grinding process [18].

Prediction and optimization of drilling parameters for Ra were investigated while drilling galvanized steel. ANFIS model with the "gbellmf" membership function produced the minimum error. The output of the ANFIS model was given as input to the GA to find the optimum process parameter. The spindle speed and tool angle was Ra's most influencing parameters [19]. Prediction of CF and Ra was carried out in the Al-20Mg_2Si-2Cu metal matrix composite with ANFIS. Feed, speed, and particle size were the inputs, and Ra was the output. The ANFIS model was suitable for forecasting the Ra with minimum error [20]. An investigation was conducted to compare the wear of ceramic tools during the machining of AISI D2 steel and glass fibre reinforced plastics (GFRP) material. The flank wear was smooth and higher for machining the GFRP, whereas low flank wear was observed while machining the AISI D2 steel [21].

An experimental study was carried out on ASTM A36 mild steel, and the wavelet denoising technique was used to decompose the noise signals, and then, the thresholding was done. The decomposed signals were trained with the ANFIS to investigate the relationship between the machining parameters and chatter. The depth of cut was the most influencing parameter on the chatter severity [22].An investigation was carried out to measure the CF, Ra, cutting power, and MRR while turning EN-GJL-250 cast iron using coated and uncoated silicon nitride ceramic tools. The study observed that Ra was affected by feed followed by speed than the depth of cut, and the CF was influenced mainly by the cutting depth followed by feed and cutting speed. ANN model was used for better prediction, and the RSM was used to identify the optimal process parameters and analyze their interactions [23]. RSM was used to perform the regression analysis and optimize the multiresponse problems [24].

Inconel 690 was machined with TiAlN-coated solid carbide insert under minimum quantity lubrication (MQL). The two models, gene expression programming (GEP) and ANN, were used to predict tool wear. The analysis reported that a speed above 100 m/min was not desirable for machining [25]. The surface morphology and chip were analyzed while turning the functionally graded (FG) specimen under nanofluid-assisted minimum quantity lubrication (NFMQL) conditions. They observed that the NFMQL method provided an ecofriendly, green, clean, and sustainable manufacturing process [26]. The tool vibration, Ra, and chip morphology was analyzed during the hard turning of hot work AISI H13 steel under multiwalled carbon nanotubes (MWCNTs) mixed nanofluid with MQL condition. They observed segmented-type serrated saw-toothed chip morphology and increased flank wear and tool vibration responsible for machined surface finish degradation [27]. The experimental investigation was carried out using Taguchi's L_{27} orthogonal array. Inconel 718 was turned with a carbide-coated insert. The Mamdani inference system with rule reduction and Sugeno subtractive clustering method was used to model the CF, in which the latter produced the minimum error [28].

Acoustic emission (AE) and CF signals were used to predict the built-up edge formation during AISI 304 stainless steel machining. The discrete wavelet and wavelet packet transform filter the noise signals. Finally, the ANFIS model was used to predict the built-up edge height [29]. A new method of diagnosing the tool wear using the stacked sparse autoencoder is proposed. The different signals obtained from various sensors like accelerometer, dynamometer, and AE sensor were used as inputs. The signals were analyzed with wavelet analysis. The accuracy of this model is 99.63%, and it is more suitable for predicting the values very shortly [30].

During the hard turning of AISI D6 steel, the responses like Ra, CF, crater wear length, crater wear width, and flank wear were measured. Different machine learning algorithms, such as polynomial regression, random forests regression, gradient-boosted trees, and adaptive boosting-based regression, were used to predict the machining characteristics. Polynomial and random forests regression performed better than other algorithms [31]. The spindle structure autoencoder wraps the signal without any parameter mining, and the high ratio compression can be transmitted with a low bandwidth cost [32]. A conditional autoencoder was applied to monitor the wind turbine blade condition. The

performance of the conditional autoencoder was compared with the classical and convolutional autoencoder methods. From the analysis, the conditional autoencoder's accuracy was higher than the other two methods [33]. A deep network method is used to forecast the tool wear with the help of motor power using the deep learning neural network theory, which can increase learning speed and enhance the training process [34].

Furthermore, most of the earlier research works exposed that flank wear was forecasted based on the control factors and CF. Many research articles have reported the prediction of flank wear during the turning operation with vibration signals using machine learning and deep learning algorithms. To the authors' best knowledge, the utilization of CF signals and turning parameters with the CAE model are not found in the literature. This work aims to develop the ANFIS and CAE model to forecast the flank wear during the dry turning of EN8 medium carbon steel. The prediction accuracy of ANFIS is compared with the CAE model.

The rest of the paper has been structured as follows: Section 2 deals with the experimental method, design of experiments, and measurement process. The modeling and prediction using ANFIS and CAE models are presented in Sections 3 and 4. The obtained results are discussed in Section 5.

2. Materials and Methods

2.1. Workpiece and Tool. The workpiece was EN8 medium carbon steel with a Brinell hardness of 255 BHN. EN8 has good tensile strength, is used for manufacturing various machine parts, and is easy to machine [35]. The TiN-coated cemented carbide tool (CNMG120408) was selected as the cutting tool. The tool insert was attached to a tool holder (PCLNR2525M12), which has a -6° of back rake angle, 5° of clearance angle, -6° of negative cutting-edge inclination angle, 95° of significant cutting edge, 0.8 mm nose radius, and 3.9 Nm of insert tightening torque.

2.2. Experimental Setup. The experiment was performed in a conventional lathe, as shown in Figure 1. The CF during the turning operation was captured using a lathe tool dynamometer. For acquiring the CF, a data acquisition system with the necessary software and hardware [36] was arranged and is shown in Figure 2.

2.3. Design of Experiments. With the help of central composite design (CCD), the effectiveness of the turning process was studied. A suitable variant in the CCD is the face-centered CCD, in which $\alpha = 1$ [37, 38]. The design matrix is presented in Table 1.

2.4. Flank Wear Measurement. Flank wear was measured with profile projector PJ-A3000 (Make: Mitutoyo). The XY measurement range and resolution were 100 mm × 100 mm and 0.001 mm, respectively. The instrument used for measurement is shown in Figure 3.

3. Modeling Using an Adaptive Neuro-Fuzzy Inference System

ANFIS is a well-known hybrid neuro-fuzzy inference system to model intricate problems was established [26]. ANFIS is a beneficial neural network (NN) method for affording the result for nonlinear and approximating functions. ANFIS employs different learning approaches to a fuzzy logic (FL) system [39].

3.1. ANFIS Prediction Model. The ANFIS catches the merits of both NN and FL principles, and the ANFIS model can efficiently and optimally forecast the response. The parameters related to the membership functions (MF) are changed through the learning process. The parameter computation is simplified by a gradient vector that measures the fuzzy inference system (FIS), which is used to model the given input/output parameters. ANFIS uses a back propagation neural network (BPNN) or a combination of least squares estimation and BPNN (hybrid) for MF parameter estimation [40]. With the help of MATLAB, the ANFIS model was developed, and the graphical user interface was used for training and testing the model.

3.1.1. ANFIS Methodology. The following steps are to be considered for developing the ANFIS model to predict flank wear:

Step 1. Define the architecture of the ANFIS.

The architecture of ANFIS is displayed in Figure 4. The input parameters, such as speed, feed, and depth of cut, were controlled, and flank wear was recorded. The corresponding cutting force was measured using the strain gauge dynamometer coupled with an amplifier and was given as one of the input parameters for the ANFIS model to forecast the flank wear. The dynamometer data were acquired using a USB 6221M series, NI DAQ Card.

Step 2. Set the input and output parameters and MF.

An MF describes how every data in the input is drawn to a membership value between 0 and 1. Several MFs are used for modeling, including trapezoidal, triangular, piecewise linear, and Gaussian. The selection of MF is based on the nature of the problem and their experience. The triangular MF was used for the distribution of the input variable. The triangular membership function (trimf) was just a curtailed triangle. It is a straight-line MF and has the benefit of easiness. The number of data points should be larger than the number of tuning parameters; hence, the three MFs were considered for every input.

3.1.2. Input and Output Parameters. There are four input parameters for the ANFIS model: speed, feed, depth of cut, and CF. Cutting speed has a significant influence on tool life. When the cutting speed increases, the cutting temperature increases, increasing the flank wear [26]. The initial MF for speed is presented in Figure 5.

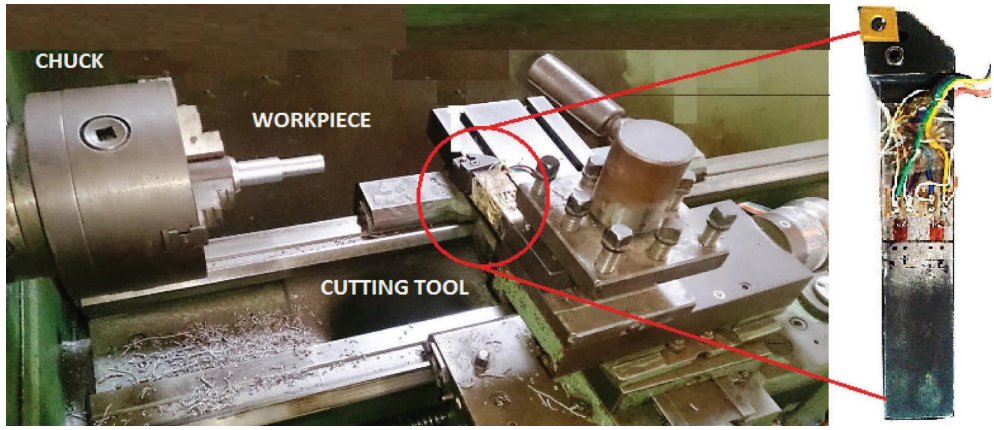

Figure 1: Cutting force measurement during the turning process.

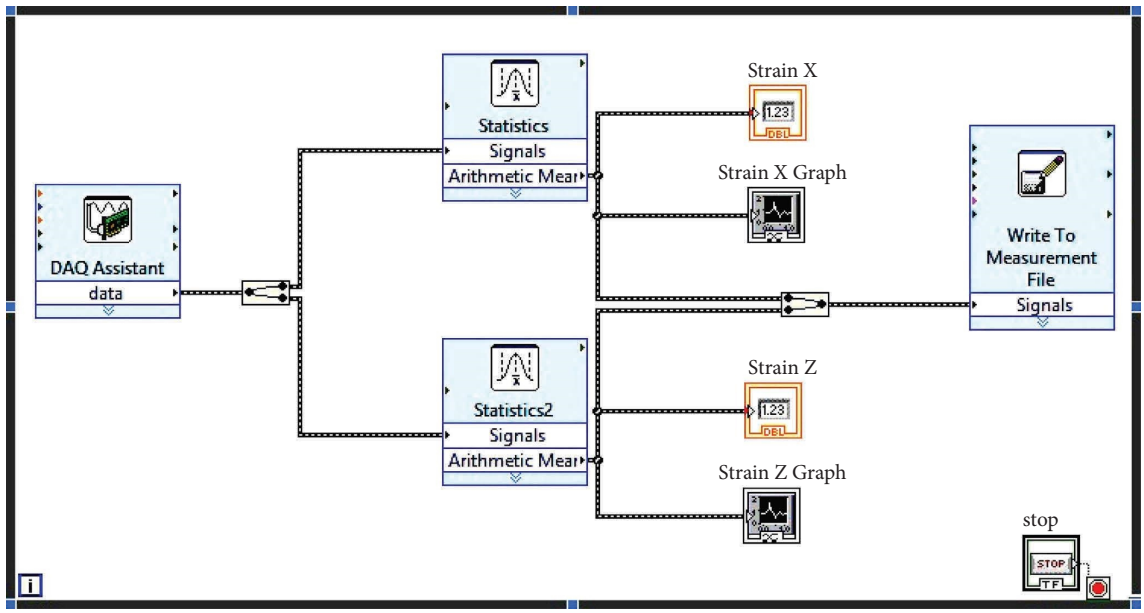

Figure 2: Illustration of signal acquisition.

Control factors and CF were considered input parameters for predicting the tool wear during this study. The CF was increased when tool wear also increased. The CF produced during the metal cutting impacted the heat generation in the cutting zone, tool wear, machined surface quality, and workpiece accuracy [27, 41].

3.1.3. Output Parameter of the ANFIS. The response of the ANFIS is flank wear which is the gradual failure of the tool due to continuous contact with the workpiece during the machining operation. The flank wear was considered as output.

Figure 6 displays the fuzzy architecture of the ANFIS model where the triangular membership function was implemented. Figure 7 is the rule editor where all the rules were fed into the fuzzy system [42]. It consists of 81 fuzzy rules (4 input parameters with three membership functions). ANFIS architecture is shown in Figure 7.

Step 3. ANFIS model training with the given input data.

For the training of the ANFIS model, 14 sets (out of 20 sets—70%) of experimental data were selected, and the training was performed with the chosen ANFIS model. The epoch was regulated until the error reached <0.001 [7]. The ANFIS learning scenario for the prediction can be analyzed from Figure 8 with epoch 20. The average error was achieved as 0.00067123 mm.

Step 4. Testing of the ANFIS model with the experimental data.

The turning data sets (6 sets—30%) obtained from the experiments were used to test with the trained ANFIS model. The response values were loaded into the ANFIS GUI and tested across the parametric value. The user can use checking data and demo data to be loaded into the GUI and can be used for prediction. Testing data was applied to the developed ANFIS model and found

Table 1: Experimental layout.

Std. order	Cutting speed (mm/min)	Feed rate (mm/rev)	Depth of cut (mm)	Cutting force (N)	Modeling
1	90	0.2	0.3	959	Training
2	270	0.2	0.3	1137	Testing
3	90	0.4	0.3	1047	Testing
4	270	0.4	0.3	1062	Training
5	90	0.2	0.6	996	Training
6	270	0.2	0.6	1084	Testing
7	90	0.4	0.6	1002	Training
8	270	0.4	0.6	1033	Training
9	90	0.3	0.45	1037	Testing
10	270	0.3	0.45	1034	Training
11	180	0.2	0.45	1042	Training
12	180	0.4	0.45	1043	Training
13	180	0.3	0.3	1040	Testing
14	180	0.3	0.6	1081	Training
15	180	0.3	0.45	1015	Testing
16	180	0.3	0.45	971	Training
17	180	0.3	0.45	1190	Training
18	180	0.3	0.45	1032	Training
19	180	0.3	0.45	997	Training
20	180	0.3	0.45	983	Training

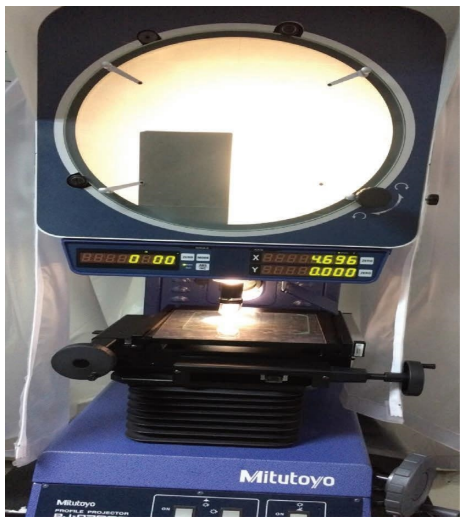

Figure 3: Profile projector for flank wear measurement.

an average error of 0.0074011 mm, shown in Figure 9. The blue circles were the actual data, and the red star was the predicted one with the same input parameters criterion.

Step 5. ANFIS model testing with experimental data.

The ANFIS model was tested with the experimental data to validate the accuracy of the model. The ANFIS can predict any value between this range. Finally, the output obtained from the ANFIS was compared with the experimental data obtained from the turning operation. The close assent displayed that the developed ANFIS can be employed to forecast flank wear. To assess the accuracy of the ANFIS model, the error E_i is defined using the following equation:

$$E_i = \frac{\text{Actual value}_i - \text{Predicted value}_i}{\text{Actual value}_i} \times 100. \quad (1)$$

4. Modeling Using Convolutional Autoencoder

Convolutional auto encoder (CAE) is an unsupervised model with convolutional layers. CAEs are typically used to reduce and compress the size of the input dimension and extract robust features. CAE is distinguished from traditional autoencoders by convolutional layers. These layers stand out for their appealing ability to extract knowledge and learn the internal representation of data. CAE system comprises two convolutional neural network (CNN) models, the encoder and the decoder. The primary function of the encoder is to convert the original input data into a lower-dimensional latent representation. The decoder is in charge of reconstructing the compressed latent representation to generate output data. Training of the CAE is nearly identical to the standard ANN. The backpropagation method minimizes the cost function and the enhanced weight and bias matrix. The structure of the purported model is shown in Figure 10. The mean square error function (MSE) and cross-entropy loss function, which can define reconstruction error, are frequently used as the cost function in autoencoder training.

The model is built in Google Colab, a free Jupyter notebook environment used to implement the CAE. Colab is a free cloud-based service provided by Google, and the best feature of Colab is that no prior installation is required.

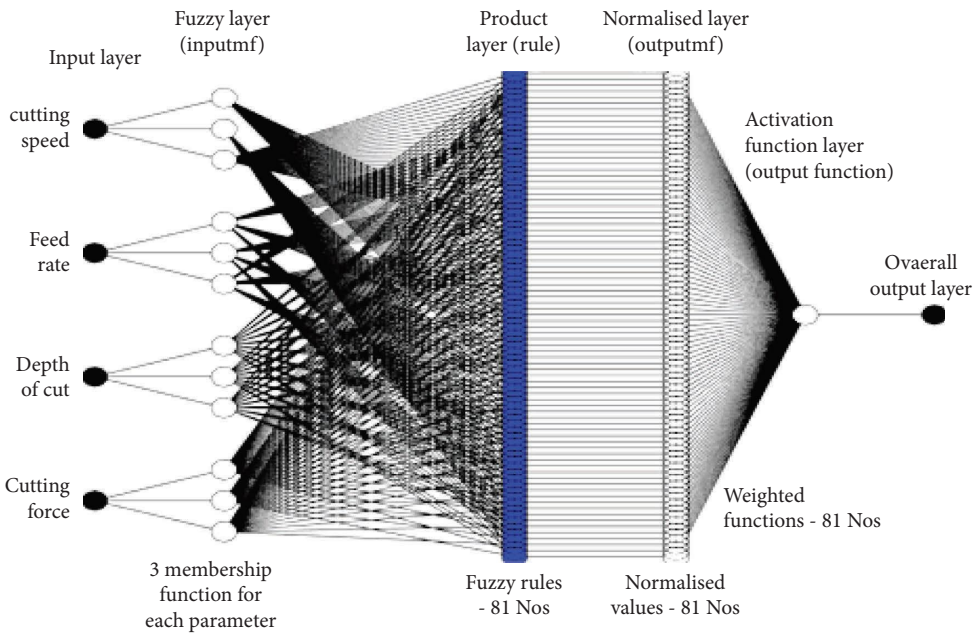

Figure 4: ANFIS structure for four input and single output parameters.

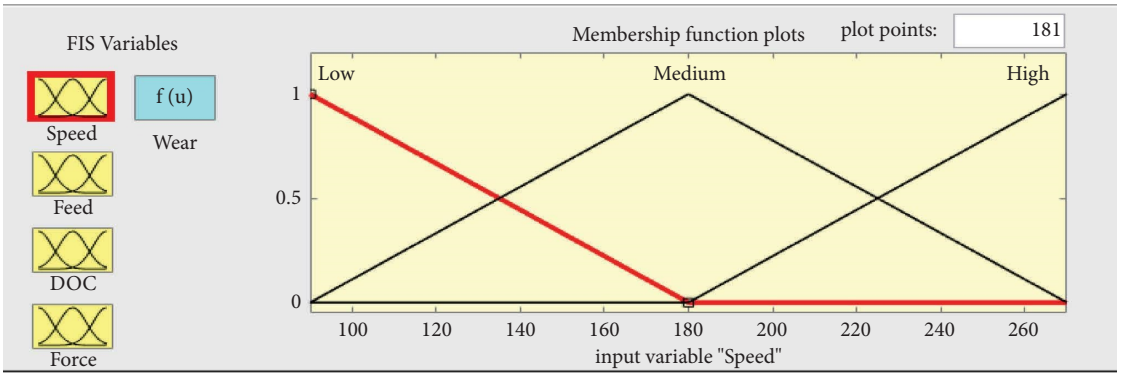

Figure 5: The initial MF for "Speed".

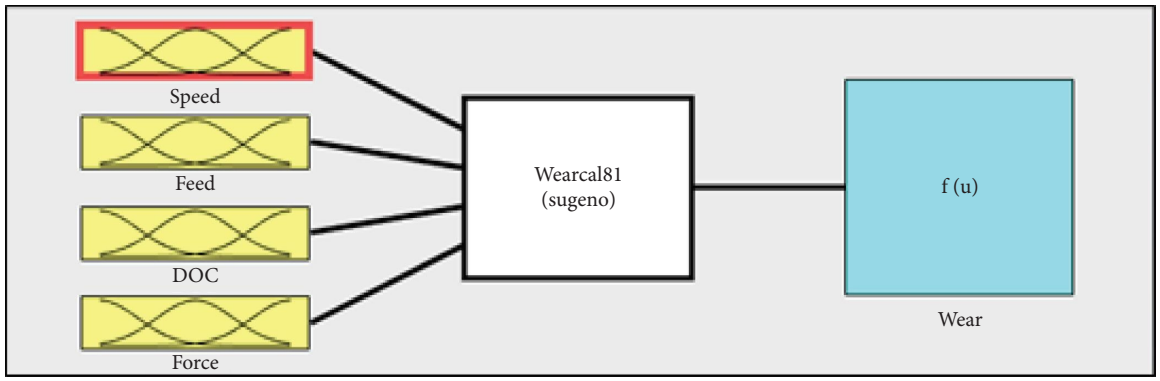

Figure 6: Architecture of ANFIS.

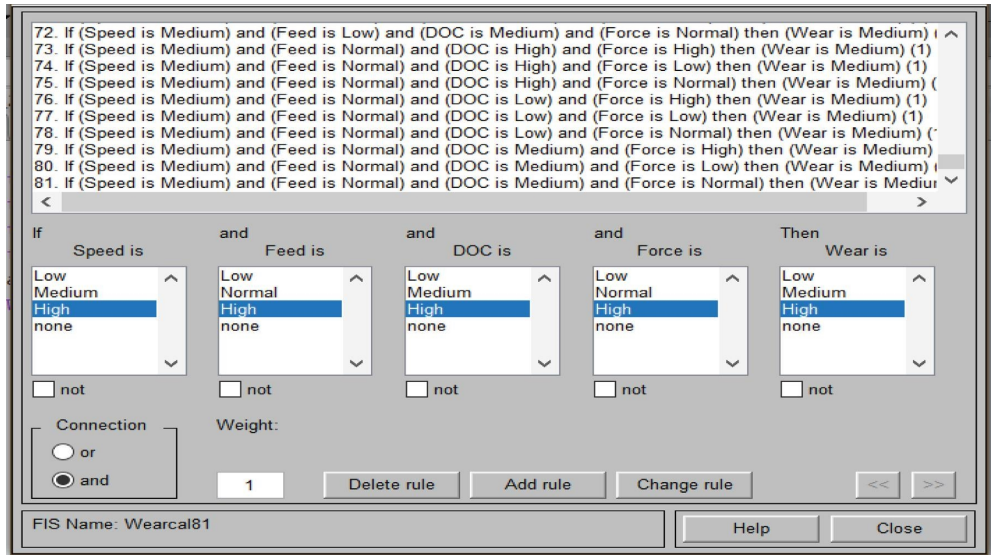

Figure 7: Rule editor.

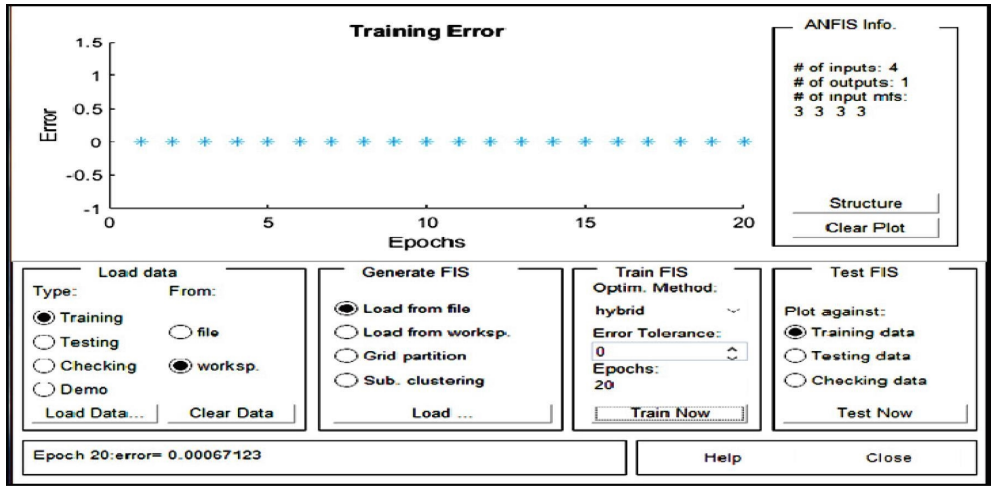

Figure 8: Training error.

Many data science and machine learning libraries are pre-installed in Colab, including Pandas, NumPy, TensorFlow, Keras, and OpenCV [43].

4.1. End-to-End-Framework. Unlike the conventional compression methods, the CAE is an end-to-end standard that combines compression and encoding methods. CAE model can persistently encode the input into small-size data by mapping the hidden layers without requiring signal transformation. Convolutional encoding (CE) and convolutional decoding (CD) are linked together during the training phase to learn mapping functions for compression and reconstruction. In CE, the input data is encoded into the compressed data as given by the following equation:

$$y = f_{w,b}(x). \tag{2}$$

In the hidden layers, x is the input signal, y is the compressed data, w is the weight, and b is the bias. In CE, $f(.)$ signifies the compression mapping function. In CD, the compressed data y are reconstructed to form the initial signal x, as defined below.

$$x = g_{w',b'}(y). \tag{3}$$

In CD, w' is the weight, and b' is the bias. The reconstruction mapping function is denoted by g(.). As a result, this end-to-end standard can condense the input to a small-scale set using the CE mapping function without an independent encoding method. Furthermore, the compressed data can be restored in CD to obtain the actual output, as shown in Table 2. It overcomes the compression quality limitation imposed by programmed expansion biases and mined parameters in conventional

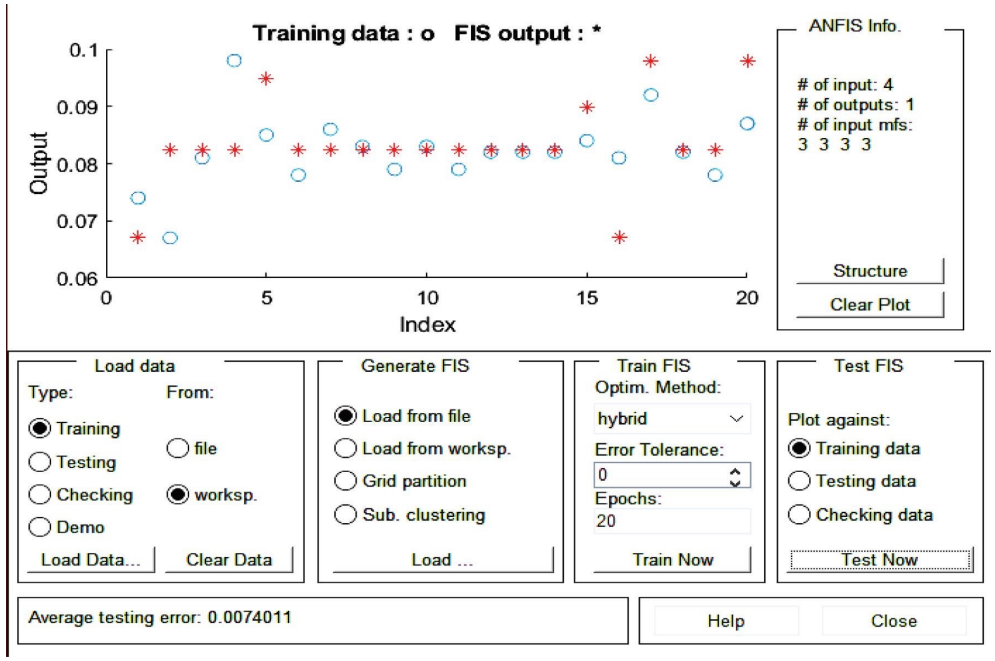

Figure 9: Testing error.

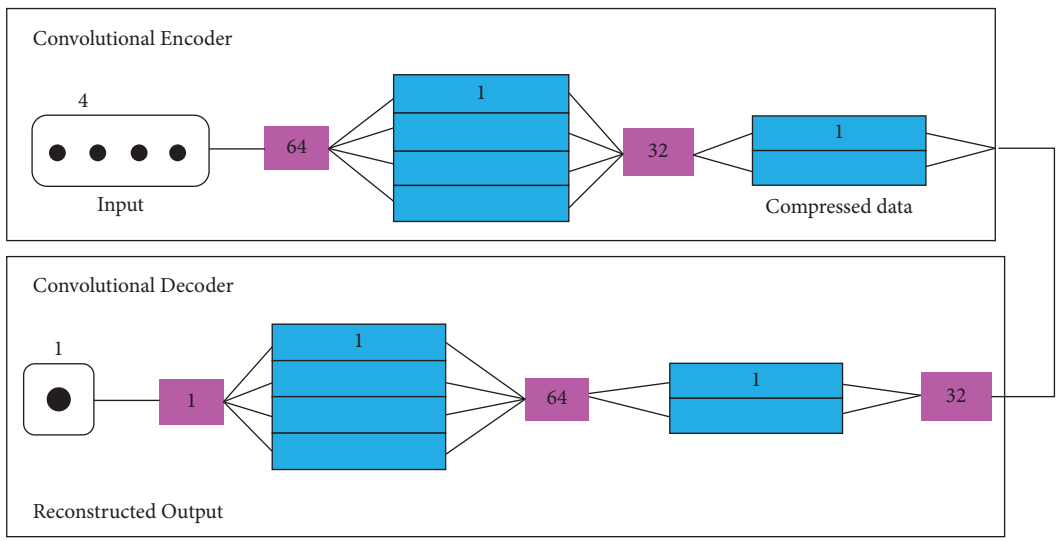

Figure 10: Structure of the CAE model.

Table 2: The details of layers and parameters using the CAE model.

Section	No	Layer name	Filters × kernels	Activation function	Output size	Parameters
CE	1	Input layer	—	—	—	—
	2	1D convolution	64 × 2	Sigmoid	(None, 1, 64)	448
	3	Dropout	—	—	—	0
	4	1D convolution	32 × 2	Sigmoid	(None, 1, 32)	4128
CD	5	1D transposed convolution	32 × 2	Sigmoid	(None, 1, 32)	2082
	6	Dropout	—	—	—	0
	7	1D transposed convolution	64 × 2	Sigmoid	(None, 1, 64)	4160
	8	1D transposed convolution	1 × 2	Sigmoid	(None, 1, 1)	129
Reconstructed output	9	—	—	—	(None, 1, 1)	—
Total no. of parameters						10,945

Table 3: Prediction accuracy of different membership functions.

S. no.	Membership function-ANFIS structure	Optimization method	Training error (mm)	Testing error (mm)
1	Gauss MF	BPNN	0.18915	1.9795
2	Gauss MF	Hybrid	**0.000134**	**0.0704**
3	TRAF MF	Hybrid	0.000966	0.0849
4	Gauss 2MF	Hybrid	0.000164	0.0783
5	PRINMF	Hybrid	0.000166	0.0788
6	DSIGMF	Hybrid	0.000165	0.0784
7	PSIGMF	Hybrid	0.000407	0.0783
8	Subtractive clustering	Hybrid	0.002239	0.0929

Table 4: Experimental vs. Predicted values.

Std. order	Flank wear (experimental)	Predicted flank wear-ANFIS	% Error	Predicted flank wear-CAE	% error
1	0.071	0.067	5.63	0.078	−9.86
2	0.067	0.073	−8.96	0.072	−7.46
3	0.081	0.083	−2.47	0.09	−11.11
4	0.098	0.093	5.10	0.08	18.37
5	0.085	0.090	−5.88	0.082	3.53
6	0.078	0.083	−6.41	0.085	−8.97
7	0.086	0.083	3.49	0.085	1.16
8	0.083	0.083	0.00	0.085	−2.41
9	0.079	0.083	−5.06	0.083	−5.06
10	0.082	0.083	−1.22	0.083	−1.22
11	0.079	0.083	−5.06	0.082	−3.80
12	0.082	0.083	−1.22	0.083	−1.22
13	0.082	0.083	−1.22	0.085	−3.66
14	0.082	0.083	−1.22	0.081	1.22
15	0.084	0.090	−7.14	0.083	1.19
16	0.081	0.077	4.94	0.082	−1.23
17	0.092	0.098	−6.52	0.083	9.78
18	0.082	0.083	−1.22	0.082	0.00
19	0.078	0.083	−6.41	0.081	−3.85
20	0.087	0.090	−3.45	0.078	10.34

ways. The end-to-end model, operated through mapping functions in hidden layers, attempts to obtain adequate compressed data that recreate the actual data with minor errors.

4.2. Training. The training of the CAE takes place using the backpropagation technique and adjusting the parameters to decrease the loss functions based on a minibatch of training models given in equation (4). The batch is randomly chosen from the training dataset. Training can be accomplished by repetitions of the forward and backward pass.

$$L = \sum_{n=1}^{N} \left(D_n - F\left(D_n\right)\right)^2, \tag{4}$$

where N is the minibatch size; D_n is the n^{th} input; $F(\cdot)$ is a function of CAE consisting CE and CD; and L is the loss function. The loss function (4) is known as the square loss, which is effective in regression analysis. Let φ be trainable matrix parameters and rules can be updated using

$$\varphi_{t+1} = \varphi_t + \frac{\eta}{N} \sum_{n=1}^{N} \nabla_{\varphi t} L\left(D_n\right), \tag{5}$$

where η is the learning rate; ∇ is the gradient operator; and t is the -training step. Parameters, including batch size and the number of iterations, impact the accuracy. After training, CAE can be divided into CE and CD to accomplish compression and restoration. The tuning parameters like w, w', b, and b' are regulated in training to curtail the modification between the restored output and actual output to attain the optimal parameter settings.

4.3. Performance Evaluation. The evaluation criteria for assessing the proposed method's reconstruction quality are mean squared error (MSE) and percentage error.

(1) Mean squared error: the mean squared error (MSE) is the standard metric for assessing the performance of most regression algorithms. The less data there are, the smaller the aggregated error, MSE, as shown in

$$L = \frac{1}{N}\left[\sum (\hat{Y} - Y)^2\right]. \tag{6}$$

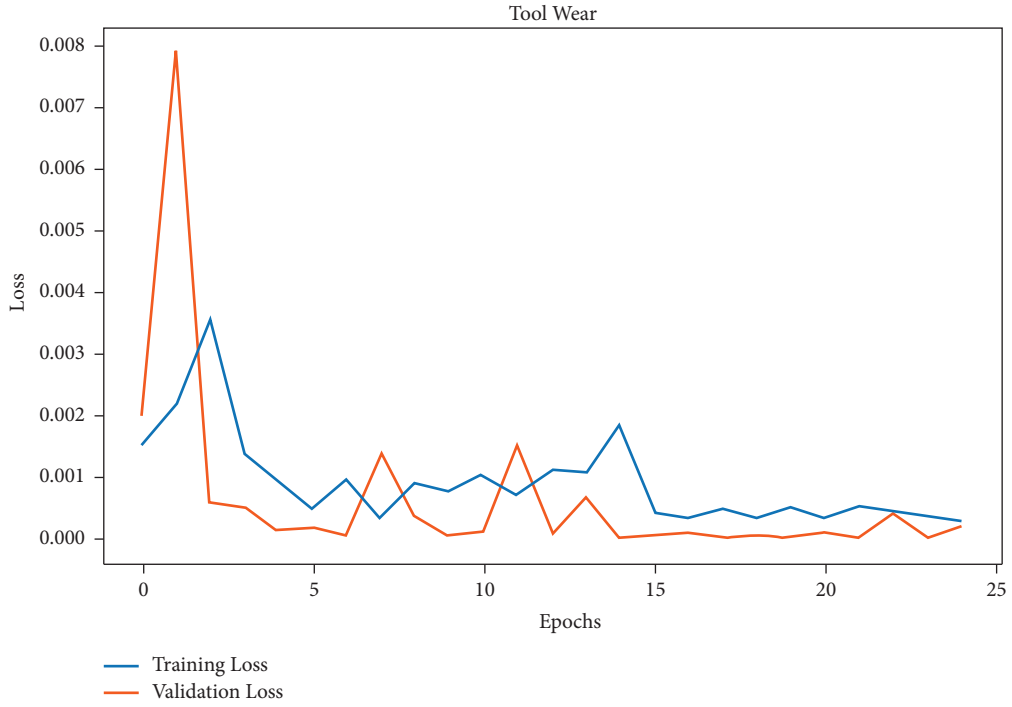

Figure 11: Fluctuation of the loss value vs. epochs for the proposed CAE.

(2) Percentage error: the percentage error is the difference between the actual and predicted values, as described in equation (7). It can be expressed as an absolute or relative error.

$$\delta = \left| \frac{\nu_A - \nu_E}{\nu_E} \right| \times 100\%. \quad (7)$$

5. Results and Discussion

The analysis was carried out between the actual data and the prediction model that depends on the various input parameters such as cutting speed, feed, depth of cut, and CF. The various MF used in ANFIS modeling reports different results. Optimizing methods like BPNN and hybrid were employed to fine-tune the membership functions. Initially, modeling was performed with the "Gauss" membership function with BPNN and the hybrid optimization method. The hybrid optimization method performed better than BPNN.

A hybrid method comprises backpropagation for the MF parameters related to the input MF. It estimates the least squares for the MF parameters connected with the output MF, which is used to reduce the error values. The grid-based ANFIS structure performed better than the subtractive clustering-based ANFIS structure; hence, grid-based model was selected [40]. The training and testing error for various MF are presented in Table 3. From Table 3, it was found that "Gauss" MF performed better than other functions. The comparison of the actual and predicted tool wear values is given in Table 4.

The CF is a significant parameter to be examined in the machining processes to determine the machined component's tool life, tool breakage, flank wear, and Ra. When the prediction value produced from the model is within the prescribed limit, the cutting tool is in satisfactory condition and can do the machining operation. If it exceeds the limit, the cutting tool is not in good condition, so it needs to be replaced. The CAE model was trained for data compression on 20 sets. Each value contains three measurements for training and three measures for validation. In the initial training phase, the model's training error reduced from 0.0035 mm to 0.001 mm during the 25 iterations. The validation error reduced from 0.008 mm to 0.001 mm during the 25 iterations, and the training error and validation error for the trails are shown in Figure 11.

6. Conclusions

The turning of EN8 steel was performed in dry conditions to accelerate the tool wear. The CF and flank wear were measured during the turning operation. The DL model was developed with speed, feed, cutting depth, and CF signals to predict flank wear. Based on the investigational results, the subsequent conclusions have arrived.

(i) Flank wear was mainly dependent on cutting speed and depth of cut.

(ii) An increase in CF indicates an increase in tool wear. Hence, CF is used as an indicator.

(iii) The hybrid optimization method performed better than BPNN in regulating the membership functions in ANFIS.

(iv) Various MFs were used to train the ANFIS model, in which the grid-based structure with Gauss MF reveals the best minimum training and testing error.

(v) Grid-based ANFIS structure performed better than subtractive clustering-based ANFIS structure.

(vi) ANFIS model was used to predict the flank wear with the minimum and maximum average error of 0.602% and 5.77%, respectively.

(vii) The overall prediction accuracy of the ANFIS model was 99.81% with the Gauss membership function.

(viii) The average prediction error for ANFIS and CAE models is 4.131% and 5.273%, respectively.

(ix) The CAE model flourishes the limitations of conventional neural networks, which arbitrarily initialize the weights of the network; hence, the proposed method can be efficiently used to predict the flank wear of the tool under various machining conditions.

(x) Compared with the conventional backpropagation method, the proposed method is more appropriate for describing the hidden wear feature from the collected data and provides better prediction accuracy.

(xi) In the future, the proposed method can monitor tool wear states online under different machining conditions. Therefore, this method is expected to be more widely used in tool wear monitoring in metal cutting processes.

(xii) For other processes like milling and drilling, the model has to be trained with selected input parameters and used to predict the tool condition.

Data Availability

The data used to support the findings of this study are included within the article.

Conflicts of Interest

The authors declare that they have no conflicts of interest.

References

[1] S. Pradhan, S. R. Das, P. C. Jena, and D. Dhupal, "Machining performance evaluation under recently developed sustainable HAJM process of zirconia ceramic using hot SiC abrasives: an experimental and simulation approach," *Proceedings of the Institution of Mechanical Engineers - Part C: Journal of Mechanical Engineering Science*, vol. 236, no. 2, pp. 1009–1035, 2022.

[2] S. Pradhan, S. R. Das, B. K. Nanda, P. C. Jena, and D. Dhupal, "Machining of hardstone quartz with modified AJM process using hot SiC abrasives: analysis, modeling, optimization, and cost analysis," *Surface Review and Letters*, vol. 28, no. 02, Article ID 2050049, 2021.

[3] L. Dan and J. Mathew, "Tool wear and failure monitoring techniques for turning—a review," *International Journal of Machine Tools and Manufacture*, vol. 30, no. 4, pp. 579–598, 1990.

[4] P. Krishnakumar, K. Rameshkumar, and K. Ramachandran, "Tool wear condition prediction using vibration signals in high speed machining (HSM) of titanium (Ti-6Al-4 V) alloy," *Procedia Computer Science*, vol. 50, pp. 270–275, 2015.

[5] T. Mohanraj, S. Shankar, R. Rajasekar, N. Sakthivel, and A. Pramanik, "Tool condition monitoring techniques in milling process—a review," *Journal of Materials Research and Technology*, vol. 9, no. 1, pp. 1032–1042, 2020.

[6] T. Mohanraj, T. Deepesh, R. Dhinesh, S. Jayaprakash, and S. Sai Krishna, "Design and analysis of a strain gauge based eight-shaped elliptical ring dynamometer for milling force measurement," *Proceedings of the Institution of Mechanical Engineers - Part C: Journal of Mechanical Engineering Science*, vol. 235, no. 17, pp. 3125–3134, 2020.

[7] T. Mohanraj, S. Shankar, R. Rajasekar, and M. Uddin, "Design, development, calibration, and testing of indigenously developed strain gauge based dynamometer for cutting force measurement in the milling process," *Journal of Mechanical Engineering and Sciences*, vol. 14, no. 2, pp. 6594–6609, 2020.

[8] M. Rizal, J. A. Ghani, M. Z. Nuawi, and C. H. C. Haron, "Online tool wear prediction system in the turning process using an adaptive neuro-fuzzy inference system," *Applied Soft Computing*, vol. 13, no. 4, pp. 1960–1968, 2013.

[9] I. Maher, M. E. H. Eltaib, A. A. D. Sarhan, and R. M. El-Zahry, "Investigation of the effect of machining parameters on the surface quality of machined brass (60/40) in CNC end milling—ANFIS modeling," *International Journal of Advanced Manufacturing Technology*, vol. 74, no. 1-4, pp. 531–537, 2014.

[10] T.-I. Liu, B. Jolley, and C.-H. Yang, "Online detection and measurements of tool wear for precision boring of titanium components," *Proceedings of the Institution of Mechanical Engineers - Part B: Journal of Engineering Manufacture*, vol. 230, no. 7, pp. 1331–1342, 2016.

[11] L. H. Saw, L. W. Ho, M. C. Yew et al., "Sensitivity analysis of drill wear and optimization using Adaptive Neuro fuzzy–genetic algorithm technique toward sustainable machining," *Journal of Cleaner Production*, vol. 172, pp. 3289–3298, 2018.

[12] B. Sen, U. K. Mandal, and S. P. Mondal, "Advancement of an intelligent system based on ANFIS for predicting machining performance parameters of Inconel 690–A perspective of metaheuristic approach," *Measurement*, vol. 109, pp. 9–17, 2017.

[13] V. Jain and T. Raj, "Tool life management of unmanned production system based on surface roughness by ANFIS," *International Journal of System Assurance Engineering and Management*, vol. 8, no. 2, pp. 458–467, 2017.

[14] I. Shivakoti, G. Kibria, P. M. Pradhan, B. B. Pradhan, and A. Sharma, "ANFIS based prediction and parametric analysis during turning operation of stainless steel 202," *Materials and Manufacturing Processes*, vol. 34, no. 1, pp. 112–121, 2019.

[15] V. Jain and T. Raj, "Prediction of cutting force by using ANFIS," *International Journal of System Assurance Engineering and Management*, vol. 9, no. 5, pp. 1137–1146, 2018.

[16] A. Khan and K. Maity, "A comprehensive GRNN model for the prediction of cutting force, surface roughness and tool

wear during turning of CP-Ti grade 2," *Silicon*, vol. 10, no. 5, pp. 2181–2191, 2018.

[17] A. Zaretalab, H. S. Haghighi, S. Mansour, and M. S. Sajadieh, "Optimisation of tool replacement time in the machining process based on tool condition monitoring using the stochastic approach," *International Journal of Computer Integrated Manufacturing*, vol. 32, no. 2, pp. 159–173, 2019.

[18] D. Nguyen, S. Yin, Q. Tang, P. X. Son, and L. A. Duc, "Online monitoring of surface roughness and grinding wheel wear when grinding Ti-6Al-4V titanium alloy using ANFIS-GPR hybrid algorithm and Taguchi analysis," *Precision Engineering*, vol. 55, pp. 275–292, 2019.

[19] R. Kumar and N. R. J. Hynes, "Prediction and optimization of surface roughness in thermal drilling using integrated ANFIS and GA approach," *Engineering Science and Technology, an International Journal*, vol. 23, no. 1, pp. 30–41, 2020.

[20] M. Marani, V. Songmene, M. Zeinali, J. Kouam, and Y. Zedan, "Neuro-fuzzy predictive model for surface roughness and cutting force of machined Al–20 Mg 2 Si–2Cu metal matrix composite using additives," *Neural Computing & Applications*, vol. 32, no. 12, pp. 8115–8126, 2020.

[21] M. A. Khan, A. S. Kumar, S. T. Kumaran, M. Uthayakumar, and T. J. Ko, "Effect of tool wear on machining GFRP and AISI D2 steel using alumina based ceramic cutting tools," *Silicon*, vol. 11, no. 1, pp. 153–158, 2019.

[22] S. Kumar and B. Singh, "Chatter prediction using merged wavelet denoising and ANFIS," *Soft Computing*, vol. 23, no. 12, pp. 4439–4458, 2019.

[23] A. Laouissi, M. A. Yallese, A. Belbah, S. Belhadi, and A. Haddad, "Investigation, modeling, and optimization of cutting parameters in turning of gray cast iron using coated and uncoated silicon nitride ceramic tools. Based on ANN, RSM, and GA optimization," *International Journal of Advanced Manufacturing Technology*, vol. 101, no. 1-4, pp. 523–548, 2019.

[24] S. Pradhan, D. Dhupal, S. R. Das, and P. C. Jena, "Experimental Investigation and optimization on machined surface of Si3N4 ceramic using hot SiC abrasive in HAJM," *Materials Today Proceedings*, vol. 44, pp. 1877–1887, 2021.

[25] B. Sen, M. Mia, U. K. Mandal, and S. P. Mondal, "GEP-and ANN-based tool wear monitoring: a virtually sensing predictive platform for MQL-assisted milling of Inconel 690," *International Journal of Advanced Manufacturing Technology*, vol. 105, no. 1-4, pp. 395–410, 2019.

[26] S. Pradhan, S. R. Das, P. C. Jena, and D. Dhupal, "Investigations on surface integrity in hard turning of functionally graded specimen under nano fluid assisted minimum quantity lubrication," *Advances in Materials and Processing Technologies*, vol. 8, pp. 1714–1729, 2021.

[27] S. Mahapatra, A. Das, P. C. Jena, and S. R. Das, "Turning of hardened AISI H13 steel with recently developed S3P-AlTiSiN coated carbide tool using MWCNT mixed nanofluid under minimum quantity lubrication," *Proceedings of the Institution of Mechanical Engineers - Part C: Journal of Mechanical Engineering Science*, vol. 237, no. 4, pp. 843–864, 2022.

[28] D. Rodić, M. Sekulić, M. Gostimirović, V. Pucovsky, and D. Kramar, "Fuzzy logic and sub-clustering approaches to predict main cutting force in high-pressure jet assisted turning," *Journal of Intelligent Manufacturing*, vol. 32, pp. 21–36, 2020.

[29] Y. Seid Ahmed, A. Arif, and S. C. Veldhuis, "Application of the wavelet transform to acoustic emission signals for built-up edge monitoring in stainless steel machining," *Measurement*, vol. 154, Article ID 107478, 2020.

[30] L. E. Escajeda Ochoa, I. B. Ruiz Quinde, J. P. Chuya Sumba, A. V. Guevara Jr, and R. Morales-Menendez, "New approach based on autoencoders to monitor the tool wear condition in HSM," *IFAC-PapersOnLine*, vol. 52, no. 11, pp. 206–211, 2019.

[31] A. Das, S. R. Das, J. P. Panda et al., "Machine Learning-based modeling and optimization in hard turning of AISI D6 steel with advanced AlTiSiN-coated carbide inserts to predict surface roughness and other machining characteristics," *Surface Review and Letters*, vol. 29, no. 10, Article ID 2250137, 2022.

[32] F. Wang, Q. Ma, W. Liu et al., "A novel ECG signal compression method using spindle convolutional auto-encoder," *Computer Methods and Programs in Biomedicine*, vol. 175, pp. 139–150, 2019.

[33] L. Yang and Z. Zhang, "A conditional convolutional autoencoder-based method for monitoring wind turbine blade breakages," *IEEE Transactions on Industrial Informatics*, vol. 17, no. 9, pp. 6390–6398, 2021.

[34] D. Wang, R. Hong, and X. Lin, "A method for predicting hobbing tool wear based on CNC real-time monitoring data and deep learning," *Precision Engineering*, vol. 72, pp. 847–857, 2021.

[35] T. Sk, S. Shankar, T. Mohanraj, and K. Devendran, "Tool wear prediction in hard turning of EN8 steel using cutting force and surface roughness with artificial neural network," *Proceedings of the Institution of Mechanical Engineers - Part C: Journal of Mechanical Engineering Science*, vol. 234, no. 1, pp. 329–342, 2020.

[36] S. Shankar, S. Thangarasu, T. Mohanraj, and D. Pravien, "Prediction of cutting force in turning process: an experimental and fuzzy approach," *Journal of Intelligent and Fuzzy Systems*, vol. 28, no. 4, pp. 1785–1793, 2015.

[37] S. Shankar, T. Mohanraj, and A. Pramanik, "Tool condition monitoring while using vegetable based cutting fluids during milling of Inconel 625," *Journal of Advanced Manufacturing Systems*, vol. 18, no. 04, pp. 563–581, 2019.

[38] J. Jena, A. Panda, A. Behera, P. Jena, S. R. Das, and D. Dhupal, "Modeling and Optimization of Surface Roughness in Hard Turning of AISI 4340 Steel with Coated Ceramic Tool," *Innovation in Materials Science and Engineering*, Springer, Berlin, Germany, 2019.

[39] M. Buragohain and C. Mahanta, "A novel approach for ANFIS modelling based on full factorial design," *Applied Soft Computing*, vol. 8, no. 1, pp. 609–625, 2008.

[40] S. Shankar, T. Mohanraj, and R. Rajasekar, "Prediction of cutting tool wear during milling process using artificial intelligence techniques," *International Journal of Computer Integrated Manufacturing*, vol. 32, no. 2, pp. 174–182, 2019.

[41] S. Shankar, T. Mohanraj, and S. K. Thangarasu, "Multi-response milling process optimization using the Taguchi method coupled to grey relational analysis," *Materials Testing*, vol. 58, no. 5, pp. 462–470, 2016.

[42] S.-I. Kwak, U.-S. Ryu, G. Kim, and M.-H. Jo, "A fuzzy reasoning method based on compensating operation and its application to fuzzy systems," *Iranian Journal of Fuzzy Systems*, vol. 16, pp. 17–34, 2019.

[43] C. Szegedy, W. Liu, Y. Jia et al., "Going deeper with convolutions," in *Proceedings of the IEEE Conference on Computer Vision and Pattern Recognition*, pp. 1–9, Boston, MA, USA, June 2015.